

# Flash Communication: Formation of a $\kappa^1$ -*o*-Diphenyl-Nickel(II) Square Planar Complex via an Oxidative Addition of 2,2'-Dibromodiphenyl to Nickel(0)

Anita Cinco, Gioele Colombo,\* Julien Furrer, Bruno Therrien, G. Attilio Ardizzoia, and Stefano Brenna\*



Cite This: *Organometallics* 2026, 45, 747–751



Read Online

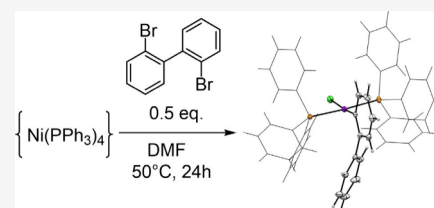
ACCESS |

Metrics & More

Article Recommendations

Supporting Information

**ABSTRACT:** This Communication describes the reaction between  $\text{Ni}(\text{PPh}_3)_4$  and 2,2'-dibromodiphenyl, leading to the isolation of an unprecedented  $\kappa^1$ -*o*-diphenyl-nickel(II) square planar complex. Full NMR characterization and the X-ray crystal structure of the title compound are reported. Preliminary investigations on the mechanism conducting to the isolated species are presented. The results of control experiments carried out using 1,1-diphenylethylene as a radical scavenger are consistent with a radical pathway rather than a double oxidative addition of the diaryl substrate. DFT calculations on the transition states involved supported these observations.



Oxidative addition of aryl halides to nickel(0) centers<sup>1</sup> is a key reaction leading to square planar nickel(II) complexes to be employed as active catalysts in numerous cross coupling reactions.<sup>2</sup> Besides nickel(II) monoaryl complexes, diaryl containing nickel(II) species also have been investigated, mainly with 1-naphthyl<sup>3–5</sup> or 2-naphthyl<sup>6–8</sup> residues. These compounds are often used as air-stable precatalysts in cross-coupling reactions or sometimes in the synthesis of Ni-anthranil or Ni-phenanthryl complexes.<sup>9</sup> Regarding nickel(II)-diphenyl compounds, Fahey synthesized 2,2'-bis[chlorobis(triethylphosphine)nickel]diphenyl (Ni-I, Figure 1)<sup>10</sup> by the reaction of  $\text{NiCl}_2(\text{PET}_3)_2$  and 2,2'-dilithiodiphenyl. In a different attempt, by reacting  $\text{Ni}(\text{COD})(\text{PET}_3)_2$  with 2,2'-dibromodiphenyl, [chlorobis(triethylphosphine)nickel]-2-diphenyl (Ni-II) was also isolated. Despite being obtained in very low yields, these species were thoroughly analyzed via <sup>1</sup>H NMR so that the very low-field doublet at about 12 ppm (Ni-I) and 9 ppm (Ni-II) could be assigned to protons H6 and H6', respectively. More recently,<sup>11</sup> Sanford et al. reported the formation of  $[\text{Ni}(\text{bipy})(\text{CH}_3\text{CN})(2-(2'\text{-F-diphenyl}))]$  (bipy = 2,2'-bipyridine) (Ni-III) as a key intermediate in the  $\text{C}(\text{sp}^2)\text{-F}$  bond-forming reductive elimination from Ni(IV) complexes.

The reported X-ray structures of diphenyl-containing nickel(II) compounds present the diaryl scaffold in different arrangements, from 2,2'-<sup>12–15</sup> or 4,4'-bridging mode,<sup>16</sup> to *m*-diphenyl<sup>17</sup> or *p*-diphenyl<sup>17,18</sup> (Figure 1). X-ray structures of mononuclear or dinuclear nickel(II) complexes having a singly bound *o*-diphenyl fragment have never been reported to date.

Herein, we investigated the reaction of  $\text{Ni}(\text{PPh}_3)_4$  with 2,2'-dibromodiphenyl, in search of the possible dinuclear diaryl nickel(II) complex 3 (Scheme 1). The nickel(0) precursor,  $\text{Ni}(\text{PPh}_3)_4$  (2), was synthesized *in situ* by reduction of  $\text{Ni}(\text{PPh}_3)_2\text{Cl}_2$  (1) with zinc dust in DMF, at 50 °C, in the presence of two additional equivalents of  $\text{PPh}_3$ .<sup>19</sup> The obtained

red suspension was then treated with 0.5 equiv of 2,2'-dibromodiphenyl and further heated at 50 °C for 24 h, during which time it changed to yellow. After workup with 2% m/m aqueous HCl<sup>20</sup> and dichloromethane, a yellow-to-orange solid stable under air and moisture was isolated. Infrared spectroscopy of the product (Figure S1) showed the presence of expected coordinated  $\text{PPh}_3$  molecules ( $1090\text{ cm}^{-1}$ ), later confirmed by a singlet resonance at 19.11 ppm in the <sup>31</sup>P{<sup>1</sup>H} NMR spectrum ( $\text{CD}_2\text{Cl}_2$ , 25 °C) (Figure S2). However, both elemental analysis and <sup>1</sup>H and <sup>13</sup>C{<sup>1</sup>H} solution NMR investigation were not consistent with the structure expected for complex 3, but they immediately revealed a different scenario. Indeed, in <sup>1</sup>H NMR ( $\text{CD}_2\text{Cl}_2$ , 25 °C) (Figure S3), a total of 39 protons were detected, thus indicating the presence of only two molecules of  $\text{PPh}_3$  in the final complex; additionally, the absence of a resonance at 123 ppm (expected for  $\text{C}(\text{sp}^2)\text{-Br}$ ) in <sup>13</sup>C{<sup>1</sup>H} NMR (Figure S4) suggested the concomitant replacement of a  $\text{C}(\text{sp}^2)\text{-Br}$  bond with a  $\text{C}(\text{sp}^2)\text{-H}$  bond on the diphenyl skeleton. Finally, elemental analysis indicated the presence of chloride instead of bromide, due to the already observed bromide-to-chloride displacement on nickel(II) centers.<sup>21</sup> Therefore, the final complex was identified as structure 4 (Scheme 1).

The nature of complex 4 was eventually confirmed by X-ray single crystal diffraction analysis: the nickel(II) center shows the anticipated square planar geometry ( $\tau_4^{22}$  and  $\tau_4^{23}$  indexes = 0.07 and 0.06, respectively), being surrounded by two *trans*-

Received: December 5, 2025

Revised: March 14, 2026

Accepted: March 19, 2026

Published: March 23, 2026



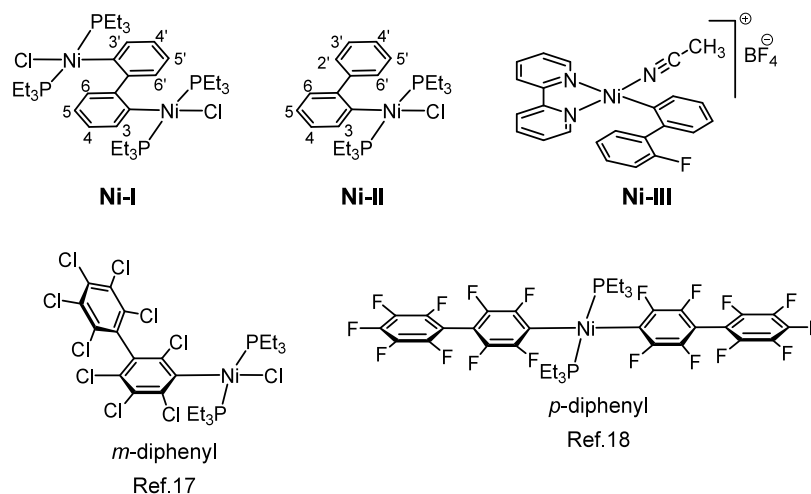
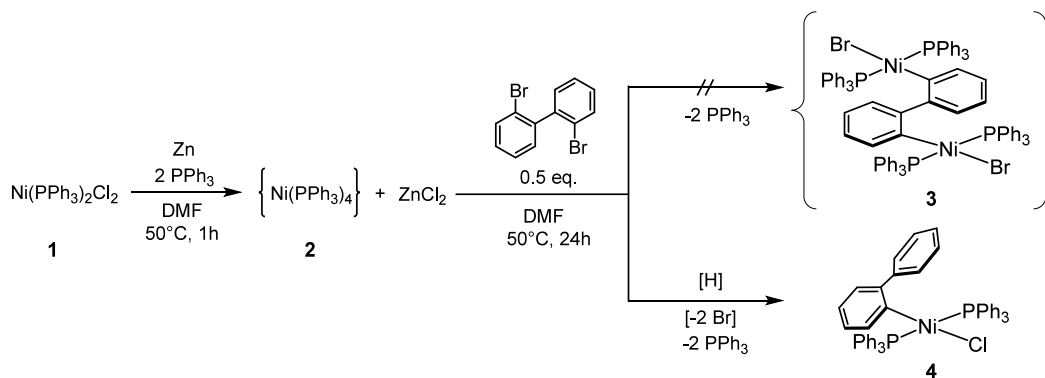


**Figure 1.** Examples of square planar nickel(II) complexes with  $\kappa^1$ -bound diphenyl fragments, either isolated (Ni-I to Ni-III) or structurally characterized (*m*- and *p*-diphenyl).

**Scheme 1. Schematic Representation of the Reaction between *in Situ* Generated  $\text{Ni}(\text{PPh}_3)_4$  and 2,2'-Dibromodiphenyl, Leading to Complex  $[\text{Ni}(\kappa^1\text{-}o\text{-diphenyl})(\text{PPh}_3)_2\text{Cl}]$  (4)**



positioned triphenylphosphines, a chloride and the  $\kappa^1$ -bound *o*-diphenyl moiety (Figure 2 and Table S1). To the best of our knowledge,  $[\text{Ni}(\kappa^1\text{-}o\text{-diphenyl})(\text{PPh}_3)_2\text{Cl}]$  (4) represents the first example of a structurally characterized mononuclear complex showing such an *o*-diphenyl residue bound to nickel(II). The torsion angle ( $\text{C}1\text{--}\text{C}6\text{--}\text{C}7\text{--}\text{C}8$ ) between the two phenyl rings in the *o*-diphenyl fragment is  $43.45(19)^\circ$  (Figure S5), which is much smaller than the corresponding values observed for the *m*- and *p*-diphenyl congeners: in the case of  $\text{C}_6\text{Cl}_5\text{C}_6\text{Cl}_4$ - derivatives,<sup>17</sup> angles up to  $87.59^\circ$  and  $89.93^\circ$  are respectively observed for *m*- $\text{C}_6\text{Cl}_5\text{C}_6\text{Cl}_4$ - and *p*- $\text{C}_6\text{Cl}_5\text{C}_6\text{Cl}_4$ - fragments, whereas in the *p*- $\text{C}_6\text{F}_4\text{C}_6\text{F}_4$ - residue<sup>18</sup> the phenyl-phenyl angle is  $53.08^\circ$ . In  $[\text{Ni}(\kappa^1\text{-}o\text{-diphenyl})(\text{PPh}_3)_2\text{Cl}]$  (4), the coordinated phenyl group of the *o*-diphenyl residue shows an angle of  $80.70^\circ$  with respect to the  $\text{NiP}_2\text{Cl}$  plane (Figure S5).

Once the nature of the final product 4 was established, we investigated the process underpinning its formation. Considering that the yield of the reaction was about 34% (based on nickel), we first searched for a possible explanation of the fate of the residual nickel. A modified workup was applied, which allowed us to identify the formation of metallic nickel in the course of the reaction. After compound 4 was obtained under standard conditions, the suspension was filtered on a pleated filter, and the solid was thoroughly washed with dichloromethane, leaving a black residue on the filter (Figure S6). The filtrate was then treated following the already mentioned workup

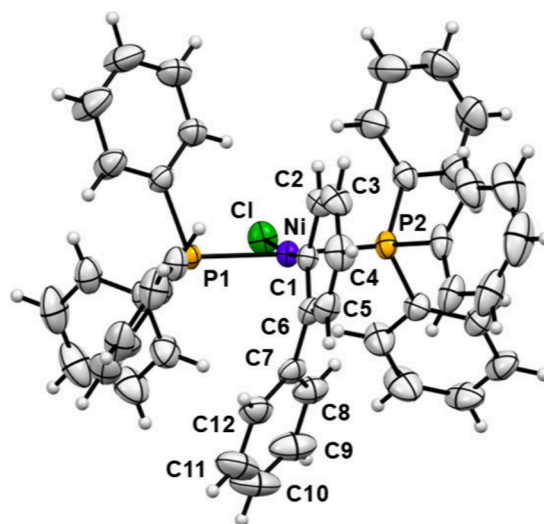


**Figure 2.** ORTEP drawing of complex 4 at the 50% probability level ellipsoids. Selected bond lengths ( $\text{\AA}$ ), angles and torsion angles ( $^\circ$ ): Ni–Cl 2.2322(5), Ni–P1 2.2282(5), Ni–P2 2.2452(5), Ni–C1 1.898(2); Cl–Ni–Cl 173.58(5), P1–Ni–P2 176.69(2), Cl–Ni–P1 90.57(2), Cl–Ni–P2 89.39(2), P1–Ni–C1 88.29(5), P2–Ni–C1 91.38(5), C1–C6–C7–C8  $43.45(19)$ .

(2% m/m aqueous HCl), allowing for the isolation of **4** in a 33% yield. The black residue in the pleated filter showed paramagnetic behavior (Figure S6), thus being designated as bulk metallic nickel(0). Reasonably, in the reduction of  $\text{Ni}(\text{PPh}_3)_2\text{Cl}_2$  to  $\text{Ni}(\text{PPh}_3)_4$  by zinc(0), a partial reduction to Ni(0) occurred. This black residue was then analyzed according to the nickel bis(dimethylglyoximate) assay,<sup>24</sup> which allowed quantification of the nickel content in the black residue as 25% (of the starting nickel). Thus, we could conclude that the nickel present in the starting  $\text{Ni}(\text{PPh}_3)_2\text{Cl}_2$  was partially converted to **4** (ca. 33–34%) and to metallic nickel (25%). The remaining nickel was reasonably converted back to  $\text{Ni}(\text{PPh}_3)_2\text{Cl}_2$  during the workup of the reaction. Also, despite it not being directly detected, the formation of  $[\text{Ni}(\text{PPh}_3)_3\text{Br}]$ , which is commonly observed as a side product in the oxidative addition of aryl bromides to Ni(0) complexes, could not be ruled out. Additionally, part of the 2,2'-dibromodiphenyl introduced is subjected to coupling reactions, as detected from GC-MS analysis of mother liquor (Figure S7). Reasonably, the presence of both nickel(0) and zinc(0) in the mixture, together with the generation of radical species in the reaction mechanism (*vide infra*) contributed to the formation of quaterphenyl or *o*-tetraphenylene products<sup>25</sup> deriving from coupling of 2,2'-dibromodiphenyl. It is also not excluded that the coupling byproducts may arise from partial decomposition of reactive intermediates or complex **4** in solution, as previously observed for  $[\text{Ni}(\text{Ph})(\text{PPh}_3)_2\text{Cl}]$ .<sup>26</sup> Worthy of note, the oxidative addition of the diaryl to  $\text{Ni}(\text{PPh}_3)_4$  in the absence of metallic zinc was also investigated: in one experiment, unreacted zinc dust was separated by cannula filtration after formation of  $\text{Ni}(\text{PPh}_3)_4$  and dilution with THF, and prior to addition of 2,2'-dibromodiphenyl. The resulting solution was then treated according to the standard procedure, affording compound **4** in 22% yield. Although compound **4** could be obtained in the absence of zinc, the lower yield observed under these conditions does not necessarily imply a direct role of zinc in the standard reaction. In this experiment, zinc removal required dilution with THF, and the solvent itself could influence the reaction outcome. Indeed, when the reaction is conducted under otherwise standard conditions but using THF instead of DMF (without removing zinc), a similarly reduced yield (19%) is observed. Thus, the solvent may influence the product distribution by affecting the relative stability of the radical species formed in the system (see below).

According to the literature,<sup>19,27–29</sup> the formation of square planar Ni(II) complexes by reaction of aryl halides to Ni(0) centers is usually explained considering two possible pathways, namely oxidative addition and radical halide abstraction. Thus, in our specific case, a double oxidative addition involving  $\text{Ni}(\text{PPh}_3)_4$  and 2,2'-dibromodiphenyl, followed by breaking of one Ni–C(sp<sup>2</sup>) bond, and a path comprising radicals were both considered. First, control experiments were carried out in the presence of radical scavengers (2,2,6,6-tetramethylpiperidine 1-oxyl, 2,2,6,6-tetramethyl-1-piperidinyloxy, TEMPO and 1,1-diphenylethylene (DPE)). Radical trapping experiments were performed using 3 equiv of scavenger relative to the aryl halide. While TEMPO is commonly employed as a radical scavenger, it is well documented that it can directly interact with Ni(0) centers, forming isolable Ni-TEMPO complexes and engaging in redox chemistry.<sup>30</sup> Consistent with these cases, the use of TEMPO in our system led to a markedly different reaction outcome, namely, the formation of a dark violet solution from which a mixture of undefined products was isolated. We attribute this to the direct interaction of TEMPO with nickel

rather than the unambiguous inhibition of a radical pathway. In contrast, when the reaction was conducted in the presence of DPE, the expected product was still formed, albeit with a dramatically lower yield (ca. 5%) compared with standard conditions. Accordingly, the interception of radical species suppresses the reaction efficiency, suggesting that a radical pathway governs the overall mechanism.

Theoretical calculations performed at the DFT/BLYP-D3(BJ) level of theory supported the statement presented above and the proposed steps of the reaction mechanism (Figure 3). Starting from  $\text{Ni}(\text{PPh}_3)_4$  (**2**), dissociation of one  $\text{PPh}_3$

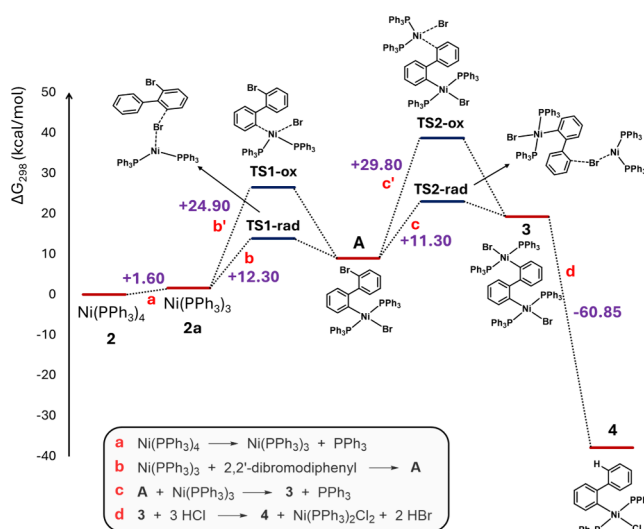


**Figure 3.** Proposed pathways explaining the formation of complex **4** via intermediate **A** and dinuclear diaryl nickel(II) complex **3**. Inset: reactions involved in each step.<sup>31</sup>

molecule to give  $\text{Ni}(\text{PPh}_3)_3$  (**2a**) likely occurs in solution ( $\Delta G_{298} = 1.60$  kcal/mol) (path a); then the first oxidative reaction at one C(sp<sup>2</sup>)–Br bond of 2,2'-dibromodiphenyl generates intermediate **A** ( $\Delta G_{298} = 7.35$  kcal/mol), either via a radical pathway through **TS1-rad** (path b) or by a three-center oxidative addition involving **TS1-ox** (path b'). According to calculated energies, the radical path is favored by 12.60 kcal/mol ( $\Delta G_{\text{TS-1rad}}^\ddagger = +12.30$ ,  $\Delta G_{\text{TS-1ox}}^\ddagger = +24.90$  kcal/mol), consistent with experimental observations on radical trapping by DPE, indicating the single-electron transfer radical pathway as dominant. A similar trend is observed also for the second C(sp<sup>2</sup>)–Br bond addition to Ni(0): intermediate **A** converts to dinuclear species **3** via a radical route (path c,  $\Delta G_{\text{TS-2rad}}^\ddagger = +11.30$  kcal/mol), which is 18.50 kcal/mol preferred compared to the classical oxidative addition (path c',  $\Delta G_{\text{TS-2ox}}^\ddagger = +29.80$  kcal/mol). The formation of compound **3** is postulated according to the seminal paper from Fahey<sup>10</sup> (see Ni-I, Figure 1). Finally, dinuclear diaryl **3** converts to complex **4** and  $\text{Ni}(\text{PPh}_3)_2\text{Cl}_2$  in the presence of excess aqueous HCl. This last reaction is particularly favorable ( $\Delta G_{298} = -60.85$  kcal/mol), thus representing a possible determining factor of the whole process. The optimized geometries of the transition states for both C(sp<sup>2</sup>)–Br bond breaking steps (**TS1-rad**, **TS1-ox**, **TS2-rad**, and **TS2-ox**) are depicted in Figure 4, whereas the *x,y,z* coordinates of all species involved are reported in the Supporting Information.

In summary, we report the synthesis and characterization of an  $\kappa^1$ -*o*-diphenyl-nickel(II) square planar complex obtained via

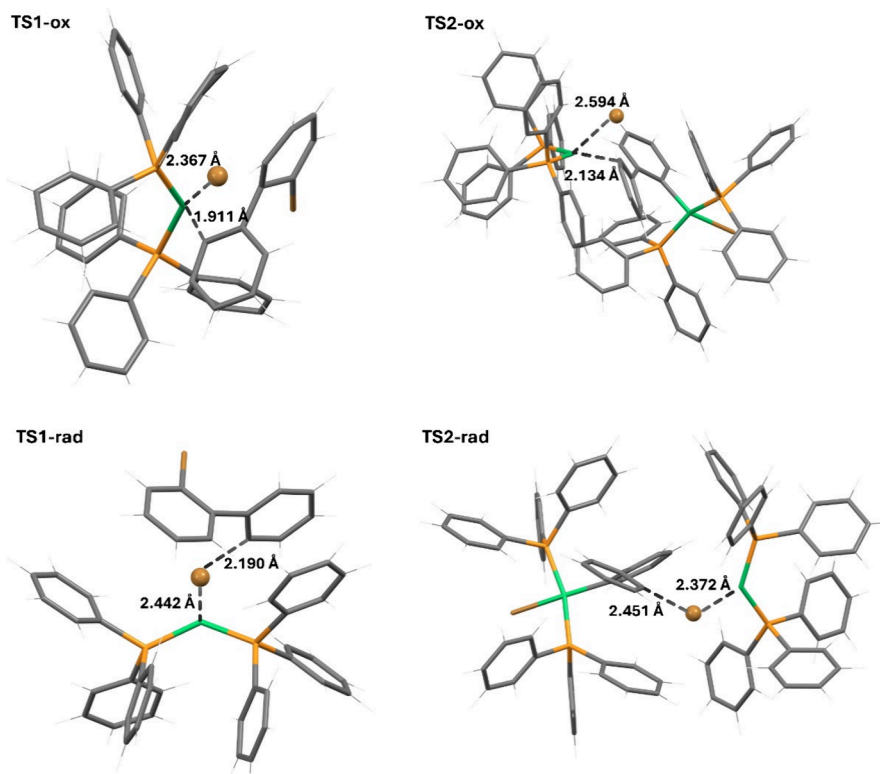


**Figure 4.** Calculated (DFT/BLYP-D3(BJ)) transition states for the formation of complex **4** after two C(sp<sup>2</sup>)–Br bond breaking steps via a radical (TS-rad) or oxidative addition (TS-ox) mechanism. Color code: nickel, green; phosphorus, orange; carbon, gray. The bromide reacting in each step is represented in ball-and-stick style.

successive oxidative addition reactions between Ni(PPh<sub>3</sub>)<sub>4</sub> and 2,2'-dibromodiphenyl. Experimental evidence and DFT calculations support a radical-type pathway operating in both C(sp<sup>2</sup>)–Br bond breaking steps of the reaction. Ongoing studies in our laboratory aim to further elucidate the full reaction mechanism and the nature of the nickel intermediate species involved. We hope these findings stimulate further investigation of *o*-diphenyl-nickel(II) square planar complexes and their potential applications.

## ■ ASSOCIATED CONTENT

### SI Supporting Information

The Supporting Information is available free of charge at <https://pubs.acs.org/doi/10.1021/acs.organomet.5c00478>.

Full experimental details, IR and NMR spectra, crystallographic data for compound **4** (PDF)

Cartesian coordinates (*xyz*) of optimized structures (tested with Mercury ver. 2024.1.0) (XYZ)

## Accession Codes

Deposition Number 2513274 contains the supplementary crystallographic data for this paper. These data can be obtained free of charge via the joint Cambridge Crystallographic Data Centre (CCDC) and Fachinformationszentrum Karlsruhe Access Structures service.

## ■ AUTHOR INFORMATION

### Corresponding Authors

Gioele Colombo – Department of Science and High Technology and CIRCC, University of Insubria, 9-22100

Como, Italy; [orcid.org/0000-0002-1096-3316](https://orcid.org/0000-0002-1096-3316);  
Email: [gioele.colombo@uninsubria.it](mailto:gioele.colombo@uninsubria.it)

Stefano Brenna – Department of Science and High Technology and CIRCC, University of Insubria, 9-22100 Como, Italy;  
[orcid.org/0000-0002-2873-2436](https://orcid.org/0000-0002-2873-2436);  
Email: [stefano.brenna@uninsubria.it](mailto:stefano.brenna@uninsubria.it)

## Authors

Anita Cinco – Department of Science and High Technology and CIRCC, University of Insubria, 9-22100 Como, Italy; University School for Advanced Studies IUSS, 15-27100 Pavia, Italy; [orcid.org/0009-0006-4386-7634](https://orcid.org/0009-0006-4386-7634)

Julien Furrer – Department für Chemie, Biochemie und Pharmazie, Universität Bern Freierstrasse 3, CH-3012 Bern, Switzerland; [orcid.org/0000-0003-2096-0618](https://orcid.org/0000-0003-2096-0618)

Bruno Therrien – Institute of Chemistry, University of Neuchâtel, CH-2000 Neuchâtel, Switzerland; [orcid.org/0000-0002-0388-2745](https://orcid.org/0000-0002-0388-2745)

G. Attilio Ardizzioia – Department of Science and High Technology and CIRCC, University of Insubria, 9-22100 Como, Italy; [orcid.org/0000-0002-7427-9919](https://orcid.org/0000-0002-7427-9919)

Complete contact information is available at:  
<https://pubs.acs.org/doi/10.1021/acs.organomet.5c00478>

## Author Contributions

The manuscript was written through contributions of all authors. All authors have given approval to the final version of the manuscript.

## Notes

The authors declare no competing financial interest.

## ACKNOWLEDGMENTS

The authors thank the Ministero dell'Università e della Ricerca (MUR) and the University of Insubria for funding. Scientific support from CRIETT Center of University of Insubria (instrument code: MAC-01, -04, -06) is greatly acknowledged.

## REFERENCES

- (1) Pierson, C. N.; Hartwig, J. F. Mapping the mechanisms of oxidative addition in cross-coupling reactions catalysed by phosphine-ligated Ni(0). *Nat. Chem.* **2024**, *16*, 930–937.
- (2) Newman-Stonebraker, S. H.; Wang, J. Y.; Jeffrey, P. D.; Doyle, A. G. Structure-Reactivity Relationships of Buchwald-Type Phosphines in Nickel-Catalyzed Cross-Couplings. *J. Am. Chem. Soc.* **2022**, *144*, 19635–19648.
- (3) Huo, J.; Fu, Y.; Tang, M. J.; Liu, P.; Dong, G. Escape from Palladium: Nickel-Catalyzed Catellani Annulation. *J. Am. Chem. Soc.* **2023**, *145*, 11005–11011.
- (4) Zhang, Z.; Niwa, T.; Watanabe, K.; Hosoya, T. 11C-Cyanation of Aryl Fluorides via Nickel and Lithium Chloride-Mediated C-F Bond Activation. *Angew. Chem., Int. Ed.* **2023**, *62*, No. e202302956.
- (5) Entz, E. D.; Russell, J. E. A.; Hooker, L. V.; Neufeldt, S. R. Small Phosphine Ligands Enable Selective Oxidative Addition of Ar–O over Ar–Cl Bonds at Nickel(0). *J. Am. Chem. Soc.* **2020**, *142*, 15454–15463.
- (6) Fujimoto, H.; Kusano, M.; Kodama, T.; Tobisu, M. Cyclization of Bisphosphines to Phosphacycles via the Cleavage of Two Carbon-Phosphorus Bonds by Nickel Catalysis. *Org. Lett.* **2019**, *21*, 4177–4181.
- (7) Cornella, J.; Gómez-Bengoa, E.; Martin, R. Combined Experimental and Theoretical Study on the Reductive Cleavage of Inert C–O Bonds with Silanes: Ruling out a Classical Ni(0)/Ni(II) Catalytic Couple and Evidence for Ni(I) Intermediates. *J. Am. Chem. Soc.* **2013**, *135*, 1997–2009.
- (8) Dubinina, G. G.; Brennessel, W. W.; Miller, J. L.; Vacic, D. A. Exploring Trifluoromethylation Reactions at Nickel: A Structural and Reactivity Study. *Organometallics* **2008**, *27*, 3933–3938.
- (9) Jezorek, R. L.; Zhang, N.; Leowanawat, P.; Bunner, M. H.; Gutsche, N.; Pesti, A. K. R.; Olsen, J. T.; Percec, V. Air-Stable Nickel Precatalysts for Fast and Quantitative Cross-Coupling of Aryl Sulfamates with Aryl Neopentylglycolboronates at Room Temperature. *Org. Lett.* **2014**, *16*, 6326–6329.
- (10) Fahey, D. R. A very low-field aromatic proton resonance in the PMR spectrum of a conformationally constrained arynickel complex. *J. Organomet. Chem.* **1973**, *57*, 385–388.
- (11) Meucci, E. A.; Ariafard, A.; Canty, A. J.; Kampf, J. W.; Sanford, M. S. Aryl-Fluoride Bond-Forming Reductive Elimination from Nickel(IV) Centers. *J. Am. Chem. Soc.* **2019**, *141*, 13261–13267.
- (12) Bennett, M. A.; Kopp, M. R.; Wenger, E.; Willis, A. C. Generation of nickel(0)-aryne and nickel(II)-biphenyldiyl complexes via in situ dehydrohalogenation of arenes. Molecular structures of [Ni(2,2'-C6H4C6H4)(dcp)] and C2-hexabenzotriphenylene. *J. Organomet. Chem.* **2003**, *667*, 8–15.
- (13) Vacic, D. A.; Jones, W. D. Modeling the Hydrodesulfurization Reaction at Nickel. Unusual Reactivity of Dibenzothiophenes Relative to Thiophene and Benzothiophene. *J. Am. Chem. Soc.* **1999**, *121*, 7606–7617.
- (14) Keen, A. L.; Doster, M.; Johnson, S. A. 1,4-Shifts in a Dinuclear Ni(I) Biaryl Complex: A Mechanistic Study of C–H Bond Activation by Monovalent Nickel. *J. Am. Chem. Soc.* **2007**, *129*, 810–819.
- (15) Keen, A. L.; Johnson, S. A. Nickel(0)-Catalyzed Isomerization of an Aryne Complex: Formation of a Dinuclear Ni(I) Complex via C–H Rather than C–F Bond Activation. *J. Am. Chem. Soc.* **2006**, *128*, 1806–1807.
- (16) Kim, Y.-J.; Sato, R.; Maruyama, T.; Osakada, K.; Yamamoto, T. Structure and Reactivity of Aryl(bromo)nickel Complexes Relevant to Nickel(0) Complex-promoted Dehalogenative Polycondensation of Organic Dihalides. *J. Chem. Soc., Dalton Trans.* **1994**, 943–948.
- (17) King, M. C.; King, R. B.; Bhattacharyya, N. K.; Newton, M. G. Organonickel chemistry in the catalytic hydrodechlorination of polychlorobiphenyls (PCBs): ligand steric effects and molecular structure of reaction intermediates. *J. Organomet. Chem.* **2000**, *600*, 63–70.
- (18) Sturge, K. C.; Hunter, A. D.; McDonald, R.; Santarsiero, B. D. Organometallic Polymer and Linear Mono-, Bi-, and Trimetallic Octafluoro-*p,p'*-biphenylene-Bridged Complexes of Bis-(methylphenylphosphine)nickel: X-ray Crystal Structures of Ni-(PMePh<sub>2</sub>)<sub>2</sub>(4,4'-C12F8H)Br and Ni(PMePh<sub>2</sub>)<sub>2</sub>(4,4'-C12F8H)<sub>2</sub>. *Organometallics* **1992**, *11*, 3056–3062.
- (19) Kende, A. S.; Liebeskind, L. S.; Braitsch, D. M. In situ generation of a solvated zerovalent nickel reagent. Biaryl formation. *Tetrahedron Lett.* **1975**, *16*, 3375–3378.
- (20) The use of a workup with aqueous HCl follows an established literature procedure for related Ni systems (see ref 19). A detailed investigation of the nickel intermediates and of all species formed during the reaction was beyond the scope of this study.
- (21) Sarker, R. K.; Mangin, L. P.; Zargarian, D. Reactivities of cyclonickellated complexes with hydroxylamines: formation of  $\kappa$ O-hydroxylamine and  $\kappa$ N-imine adducts and a  $\kappa$ O,  $\kappa$ N-aminoxide derivative. *Dalton Trans.* **2023**, *52*, 366–375.
- (22) Yang, L.; Powell, D. R.; Houser, R. P. Structural variation in copper(I) complexes with pyridylmethylamide ligands: structural analysis with a new four-coordinate geometry index,  $\tau_4$ . *Dalton Trans.* **2007**, 955–964.
- (23) Okuniewski, A.; Rosiak, D.; Chojnacki, J.; Becker, B. Coordination polymers and molecular structures among complexes of mercury(II) halides with selected 1-benzoylthioureas. *Polyhedron* **2015**, *90*, 47–57.
- (24) (a) Tschugaeff, L. Über ein neues, empfindliches Reagens auf Nickel. *Ber. Deutsch. Chem. Ges.* **1905**, *38*, 2520–2522. (b) Williams, D. E.; Wohllauer, G.; Rundle, R. E. Crystal Structures of Nickel and Palladium Dimethylglyoximes. *J. Am. Chem. Soc.* **1959**, *81*, 755–756.
- (25) Irgartinger, H.; Reibel, W. R. K. Structures of Dibenzo[*a,e*]-cyclooctatetraene and Tetrabenzo[*a,c,e,g*]cyclooctatetraene (o-Tetra-phenylene). *Acta Crystallogr.* **1981**, *B37*, 1724–1728.
- (26) Manzoor, A.; Wienefeld, P.; Baird, M. C.; Budzelaar, P. H. M. Catalysis of Cross-Coupling and Homocoupling Reactions of Aryl Halides Utilizing Ni(0), Ni(I), and Ni(II) Precursors; Ni(0) Compounds as the Probable Catalytic Species but Ni(I) Compounds as Intermediates and Products. *Organometallics* **2017**, *36*, 3508–3519.
- (27) Funes-Ardoiz, I.; Nelson, D. J.; Maseras, F. Halide Abstraction Competes with Oxidative Addition in the Reactions of Aryl Halides with [Ni(PMenPh(3-n))<sub>4</sub>]. *Chem.—Eur. J.* **2017**, *23*, 16728–16733.
- (28) Tsou, T. T.; Kochi, J. K. Mechanism of Oxidative Addition. Reaction of Nickel(0) Complexes with Aromatic Halides. *J. Am. Chem. Soc.* **1979**, *101*, 6319–6332.
- (29) Pierson, C. N.; Hartwig, J. F. Mapping the mechanisms of oxidative addition in cross-coupling reactions catalysed by phosphine-ligated Ni(0). *Nat. Chem.* **2024**, *16*, 930–937.
- (30) Isrow, D.; DeYonker, N. J.; Koppaka, A.; Pellechia, P. J.; Webster, C. E.; Captain, B. Metal-Ligand Synergistic Effects in the Complex Ni( $\eta^2$ -TEMPO)<sub>2</sub>: Synthesis, Structures, and Reactivity. *Inorg. Chem.* **2013**, *52*, 13882–13893.
- (31) Calculations were performed according to the modified workup (i.e., filtration of the mixture on a pleated filter to remove nickel(0) formed and washings with dichloromethane). In this way, nickel(0) was excluded from the reactions reported in the inset in Figure 3.